

TECHNICAL DEVELOPMENTS

THE COMPUTATIONAL FACILITIES OF THE LAB

R. Au, R. Fox, B. Pollack

Abstract

This paper describes the computational facilities at NSCL. Special attention is given to the expected function of each of the computer systems. The paper only deals with computational facilities available to the physics community and explicitly ignores the accelerator control system which is discussed in another submission.

1.0 INTRODUCTION

The computational facilities made available at NSCL were put together with the idea that several specialized computer configurations could meet the needs of the lab and user community far more cost effectively than a single general purpose computing system. Thus, we decided to purchase several large (32-bit) minicomputers and configure each for only a limited set of roles. In this paper, we describe the computing environments which are present at NSCL. We will then give a brief description of each system and show how it has been configured to match its task.

2.0 COMPUTING ENVIRONMENTS AT NSCL

Computing environments at NSCL cover a broad variety of applications. These applications range from high speed data acquisition to compute intensive batch jobs. Each application has a different set of data processing requirements. In the two extremes, high speed data acquisition requires a machine which is extremely responsive to real time events, while batch jobs typically require either a large physical memory, a fast central processor, or both.

It is possible to identify several computing needs and characterize their machine requirements. In particular:

1. Data acquisition: Requires a machine responsive to real time events. Requires the ability, depending on the complexity of the experiment, and the associated on-line analysis algorithms, to dedicate an entire computer. Requires, depending on the number and type of spectra accumulated, large amounts of physical memory. Requires special purpose interfaces to data acquisition hardware such as CAMAC crates and high resolution graphics devices.
2. Data analysis and reduction: Requires a great deal of physical memory. Requires a large number of computing cycles. Does not require a high degree of real time responsiveness, although for early stages of reduction,

interactive responsiveness is quite useful. Requires a large, fast, random access data storage system in order to reduce the time spent waiting for I/O to complete while sorting raw event data.

3. Run preparation: Requires a large number of compute cycles and interactive responsiveness.
4. Cyclotron and beam line design: Requires a large number of compute cycles. Some applications, such as magnet relaxation codes, require large amounts of physical memory.
5. Theoretical model codes or 'computer experiments': These typically require an immense number of compute cycles. They will often require large amounts of physical memory and large amounts of offline mass storage.
6. Administrative programs: Typically require interactive response times and large databases stored on offline mass storage.
7. Program development: Requires interactive response times. Does not require immense CPU or data storage capacity. Sometimes requires exclusive use of a computer such as when debugging privileged codes which could be dangerous to system integrity. Requires special interface hardware to allow the development of data acquisition codes. This interface hardware should be unable to influence the normal data acquisition system hardware.

3.0 COMPUTING FACILITIES PROVIDED

The computing facilities of NSCL consist of several 32-bit VAX minicomputers. In this section, we discuss the configuration of each system and show how it contributes towards that system's primary function. It is important to note that each of these systems is a complete computer system and that work not related to each system's primary function is not excluded, but takes place at a rate determined by the resources available. This overlap is a protective measure which allows work to go on in spite of maintenance periods or computer failure.

The computing facilities at NSCL consist of one VAX-780 minicomputer and four VAX-750 minicomputers. Both the 750 and 780 are 32-bit minicomputers. The two computer types are software compatible, given adequate hardware resources. The VAX-750 is a scaled down version of the VAX-780. The VAX-750 is one third as fast as the VAX-780, and is limited to 8Mbytes of physical memory. The I/O structure of the VAX-750 is, however, one more suitable for realtime devices than that of the VAX-780. The VAX-750 is also less than half the price of a VAX-780.

We will now proceed with a detailed examination of each of the computer systems available at NSCL. We have named each system

after its primary function, TEST, DATA1 DATA2, ANALYSIS, and VAX. These names are also used as keywords to a terminal switching network which allows any of the more than fifty terminal in the lab to access any of the computer systems.

3.1 TEST

The TEST machine is used primarily for program test and development. It is also available to CPU intensive programs. The TEST machine is a VAX-750 with 2Mbytes of physical memory, 120MBytes of disk, dual density tape drives (800/1600bpi) and a writable control store (Micro program store). It is also equipped with the lab standard data acquisitions interface, a CAMAC serial highway driver (Kinetic Systems Model 2050).

The TEST computer is used to test new CAMAC hardware. It is also used by the detector lab for detector development work. It is used by the programming staff for the development of new data acquisition software. In this capacity, it may be temporarily shut down from time to time. New system software supplied by the computer manufacturer is also first installed on this machine for a shakedown period. Recently, this system was also used to map the first harmonic field distortions in the K-500 cyclotron.

We hope to use the writable control store to develop extensions to the VAX instruction set which would streamline data acquisition and analysis. At this time, however, the writable control store contains microcode which implements a set of extended range and precision instructions. This makes TEST an attractive machine for programs which come to the lab from computers having numerical representations which allow numbers of extended range and precision.

3.2 DATA1 And DATA2

The use of these computers is covered in detail in the paper: "Status of Data Acquisition System Development" in another part of this publication. Each of these computers is used for high speed data acquisition and final experiment setup. These machines are VAX-750's with 3Mbytes of physical memory, 400Mbytes of disk storage, dual density tape drives (1600/6250), color graphics terminal, and a data acquisition interface to one of the two experimental electronics setup areas.

These systems are dedicated to individual, scheduled experiments. Typically one computer will be allocated to the group currently running, while a second is allocated to the group next scheduled to run. The priority system and working sets are assigned such that other work may be done on these machines only on a time and space

available basis. The amount of time available for other work varies drastically as function of the data rate and the complexity of the online analysis being performed.

3.3 Analysis

This system is a VAX-750 configured with 3Mbytes of physical memory, 800Mbytes of disk storage, two dual density tape drives (1600/6250), color graphics terminal, and floating point accelerator. This machine is primarily used for off line data analysis. Some cyclotron computations and some non compute intensive theoretical calculations are also done on this system. The large disk storage facility allows the temporary storage of some event tapes which greatly speeds the process of event data analysis.

A word should be said about the allocation of disk space, which is divided physically into two 400Mbyte disks. The first is used as a user disk. A quota is enforced on the amount of space each account may use. The second is a combination system disk and short term loan disk. Those tasks which require storage in excess of the quota available on the user disk may sign out space on this disk on a first come first serve basis.

3.4 VAX

As the generic name implies, this computer is the catchall system. It is a VAX-780 configured with 4Mbytes of physical memory, 1300Mbytes of disk storage, a dual density tape drive (1600/6250) and a floating point accelerator. The disks are divided by useage. One disk (400Mbytes) is reserved for the theory group which is responsible for space control. The second disk (400 Mbytes) is a user disk which contains the programs and files for all other users of this computer, it is completely analogous to the user disk on the ANALYSIS computer. The last disk (500Mbytes) is used for a combination system and short term loan disk.

The jobs run on this computer include large compute and memory bound jobs, some data reduction, cyclotron computations, word processing, and administrative data base manipulations (purchase order system).

4.0 CONCLUSIONS

The concept of a division of labor among several specialized computer systems, each one configured to best handle a small subset of the computational load, has proved a cost effective solution to computing problems which are faced by an installation such as NSCL.

STATUS OF DATA ACQUISITION SYSTEM DEVELOPMENT

R. Au, R. Fox, D. Notman, B. Sherrill

Abstract

The current state of the NSCL data acquisition system is reported. Special attention is given to the hardware and software configuration of the system as it currently runs. A short segment will be devoted to the plans for future expansion and development.

1.0 INTRODUCTION

The data acquisition system at NSCL must cater to a wide variety of experiments ranging from fixed event length spectrograph experiments, variable length multiparameter experiments, multiplicity experiments involving sparse data scans of the data acquisition hardware, and in the future, 4π solid angle detector arrays and track recording systems. During the past year, we have brought up several hardware and software components which will serve as building blocks for the development ahead. This paper will give an account of the progress to date in on line data acquisition.

The data acquisition system at NSCL is based on a multiprocessor, multitasking philosophy. We use a VAX-750 minicomputer with an LSI-11/23 as a front end data capture device. The software in both of these computers is multitasking. The LSI-11 not only takes event data, but has programs which are responsible for run control, and the accumulation, and live display, of a number of scalars. The VAX software includes programs which display accumulated histograms as well as programs which are responsible for binning the raw event data. 2.0.

HARDWARE CONFIGURATION

The data acquisition system consists of a pair of identical computer systems. Typically, one of these is taking data from the current cyclotron experiment, while the other is being used for experiment set up. The system taking data is at the complete disposal of the experimental group, while the set up machine is available to other users. When an experiment ends, the system which has been taking data switches roles with the system which has been used for set up. The data acquisition hardware can be roughly divided into two sections, main computer and data capture.

Each of the main data acquisition computers is a VAX-750 configured with 3Mbytes of physical memory, 400Mbytes of rotating disk storage, and a dual density (1600/6250bpi) tape drive. The VAX's

are also interfaced to some rather specialized data acquisition hardware. A Kinetic Systems model 2050 CAMAC serial highway driver provides the interconnection between the VAX and the associated experimental data capture hardware. The spectra accumulated on line are displayed on an Advanced Electronics Design model 512 color graphics terminal. This terminal is capable of displaying monochrome one dimensional histograms and color density plots of two dimensional spectra with 512x512 channel resolution.

The serial CAMAC highway connects the VAX to the data capture hardware. This consists of an LSI-11/23 which is resident in a CAMAC crate, and the usual assortment of scalars, ADC's, TDC's, and QDC's. The LSI-11/23 has at its disposal a terminal, which is used during experimental runs to keep a live display of several scalars as well as debugging the LSI code during the test phase. The LSI-11 is interfaced to two CAMAC crates via controllers of vastly different architectures. One of these controllers maps the CAMAC crate into the I/O page of the LSI-11 which facilitates sparse data scans of the devices in that crate. The other controller is a block mode DMA controller which provides a low overhead interface to devices which operate in a block transfer mode such as the LeCroy PCOS data bus interface, as well as a method to scan down several modules in a single crate (Q-scan mode) which is used to read live time scalars.

The VAX and LSI-11 communicate via a CAMAC dataway/Q-bus interface which gives the VAX DMA access to the LSI-11 memory through CAMAC function codes. In normal operation, the LSI-11 will buffer up event data or scalar data and notify the VAX that data is ready to be taken via a serial graded LAM (SGL). The LSI also loads the address register of the CAMAC/Q-bus link. The VAX, on receipt of the SGL, then issues a block read which transfers the buffer to the VAX. When the transfer is complete, the VAX signals receipt of the buffer to the LSI-11 by resetting the SGL and causing the dataway/Q-bus interface to generate a local LAM within the LSI-11 crate.

3.0 LSI-11 SOFTWARE CONFIGURATION

The software in the LSI-11 runs under the auspices of a multitasking system developed by D. Notman at NSCL. This system, called DATEX for DATA acquisition EXective, supports a low overhead event driven scheduler. Processes may be blocked waiting resources, or event flags, or may voluntarily relinquish the CPU. Interprocess communication is supported through pipeline like internal pseudo devices. There is primitive support for timer requests as well as a concept of device register ownership to ensure device/program synchronization.

The software in the LSI-11 is divided into several interacting processes. Space only permits a brief list of these processes and their functions.

1. VAX Comm. -- This process is responsible for sending buffers of data to the VAX from the LSI-11. It receives buffers through a pipeline, sends them to the VAX and then returns the buffers to the sender through a return pipeline specified by the sender.
2. Scaler display -- This process receives buffers of scaler data through a pipeline and interacts with a terminal to produce live scaler displays. It passes the data buffers in turn to VAX comm. for transmission to the VAX. A section of this program must be altered for each experiment.
3. Scaler reader -- This process periodically reads a set of CAMAC scalers via a Q-scan with the DMA crate controller. It sends these buffers of data to the Scaler display process.
4. Event reader -- This program fills buffers with event data and sends them off to the VAX via the VAX Comm. program. A section of this program must be altered for each experiment.
5. Acquisition control -- This program interacts with a set of switches to control the start and stop of data acquisition.

4.0 VAX SOFTWARE CONFIGURATION

The VAX is used for the actual on line analysis and event taping of data buffers sent to it by the LSI-11. At present, three software components are of importance. The first is a VAX/VMS device driver which allows programs to communicate with the CAMAC system. The second is a histogram display program which takes histograms out of a shared common region and displays them as instructed on the AED-512 color graphics terminal. The final program is a user written acquisition program which takes data from the CAMAC and produces histograms which the AED program displays.

The VAX/VMS CAMAC device driver is a list processing device driver written by R. Au. It takes lists of CAMAC commands, and control information and interprets them into 2050 operations. Some of the operations supported by hardware and this software include Q-scan's of crates, Block mode transfers, Wait for selected SGL, loop on a CAMAC instruction list, and single shot CAMAC commands.

The AED display program, also written by R. Au, is responsible for presenting the histograms accumulated on line. It is able to display up to

128 histograms of arbitrary dimensions totaling up to 1Mbyte of storage. Byte, INTEGER*2 and INTEGER*4 histograms are supported. The AED program runs as a detached process, independent of the histogramming program. It may send data back to the histogramming process by means of a mailbox. The data sent can include such things as command characters, selected points, or sets of points. It can independently select gates and bands, integrate regions, do expansions and set up multiple display pictures. The histogramming program can send some text and primitive graphic data to the program to be displayed.

The histogramming program is one which varies from experiment to experiment, although some effort is being made to standardize large sections of it. In theory any program capable of reading the CAMAC, and producing histograms may be used here, but in fact, time typically does not permit the construction of a program from scratch for each experiment. Fortunately, many experiments can use the same skeleton program, only changing the histogramming, or parameter extraction sections. Two histogramming program skeletons are in popular use at NSCL. One, written by B. Sherrill, is suitable for spectrograph and other fairly fixed length event experiments. The other, written by a collaboration of G. Westfall, B. V. Jacak, L. Harwood, and R. Fox is used typically where the event stream contains variable length events.

5.0 FUTURE DEVELOPMENTS

Developments planned for the future must address the drawbacks of the current data acquisition system. The current data acquisition rates (~2,000 parameters/sec) are insufficient to meet the projected rates for future experiments, the bottleneck appears to be the LSI-11 execution speed. Another, far more insidious, bottle neck exists in the programming effort required to bring up the software for each new experiment.

We hope to address the acquisition rate problem by a direct substitution of a multiprocessor array based on the motorola 68000 series microprocessor. In this array, each processor is from 3-5 times faster than the LSI-11. Additionally, when used in a multiprocessor array, will overlap both transmission and formatting in one processor with event acquisition in the others.

The software bottle neck is being addressed by an extension of the multiprocessing philosophy. The idea here is to provide a routing program which shoots buffers around to a number of programs. These programs would be a mixture of standard programs, and user tailored programs. Histogramming would be done in two stages. the first stage would be a user written subroutine in

a lab provided skeleton which unpacks the buffer into a set of parameter tables. The parameter tables are then sent on to a general histogramming package which performs the gating and histogram generation. Thus, we hope to reduce the individual programming effort in the VAX to a single user written subroutine.

6.0 CONCLUSIONS

The data acquisition system has been running now since Sept. 1982. In this, the first run period, we have gained quite a bit of experience with the strengths and weaknesses of the system. We have formulated a more detailed picture of the development of the system in the year to come. It is only through continued examination of the ways in which the system is being used and being stressed that we will be able to approach a flexible, usable, powerful data acquisition system.

STATUS OF CONTROL SYSTEM SOFTWARE DEVELOPMENT

R. Au, R. Fox, B. Jeltema, B. Johnson

Abstract

The current status of the control system for the k-500 cyclotron is discussed. An overview of the hardware and software configuration are also given.

1.0 INTRODUCTION

At an early stage in the K-500/K-800 planning, it was decided that these devices should be computer controlled. We felt that in view of the number of devices which are involved, and in view of the expense of cabling these devices to a central location, as would be required for a hard wired control system, computer control would in the long run be far more cost effective, and more flexible than a similar hard wired system.

The following response requirements strongly influenced the development of the project.

1. Approximately 1000 devices would be controlled by the final system. This included all devices on the K-500, K-800 cyclotrons as well as the associated beam lines and experimental facilities.
2. It should be possible to distribute the control areas so that physicists could control the portions of the experimental facilities which were involved in their experiments.
3. It should be possible to have multiple control devices attached to a controlled device (this is a direct consequence of the previous requirement).
4. Response to the operator should be in real time (~.1 seconds).
5. The system would look to the operator primarily like a hard wired control system with the exception of a very few 'smart' controllers or other smart functions. In particular, the use of knobs and meters for control and display devices was deemed superior to traditional computer input devices such as keypads and terminals.

The first section below gives the final computer hardware configuration as far as it influences the control system software development. The next section gives an overview of the software strategy used, while the last section gives summary of the development so far.

2.0 COMPUTER HARDWARE

The control system hardware finally chosen was based on a tightly coupled multiprocessor system. Each of the processors was chosen from

the DEC PDP-11 family of minicomputers and had a specific set of duties to perform. Communications between the processors was by means of a shared multiport memory.

The processors chosen were two PDP-11/34's, and one PDP-11/45. The two 11/34's run as stand alone controllers for the console apparatus and the cyclotron apparatus, while the 11/45 performs general overseeing functions, and serves as the program development machine. The 11/34's run in a stand alone environment using the RSX-11S operating system. The RSX-11S system is a diskless variant of the RSX-11M system, which is run on the 11/45. Thus, the 11/45 possesses all of the mass storage devices (disks, tape drives), of the control system as well as the traditional input/output equipment (terminals, graphics displays and so on). All computers are equipped with 124Kw of memory with parity error detection. The processors communicate via 16Kw of 4-port memory. The control computers communicate with the outside world via a CAMAC serial highway which talks to the control computers via a Kinetics Systems Model 2050 serial highway driver. This device is a list processing DMA interface to a CAMAC serial highway (ANSII/IEEE Std 595-1982). To use it one sets up lists of valid CAMAC commands and points the 2050 at them. The output data is taken from the list, while the input data is placed in a data list.

The control system serial highway is topologically a two loop system. The console devices reside on one loop accessible to only the console 11/34, while the cyclotron devices reside on a second loop accessible only to the cyclo 11/34. The 11/45 can only directly talk to some K-500 main magnet monitoring devices.

3.0 CONTROL SYSTEM SOFTWARE

The basic software strategy has been to keep an up to date map of the control system status available at all times in the multiport memory. The console 11/34 is obligated to maintain the set of cells in the multiport memory corresponding to the values that are requested of the control devices, and is also responsible for monitoring the actual value cells in the multiport and displaying them on the console displays. The cyclotron 11/34 has similar obligations except that it must update the actual values in the multiport and use the requested values in the multiport to alter the condition of the control hardware. The control system software is divided logically in several segments.

1. Control software for the console (entirely in the console 11/34).
2. Control software for cyclotron devices (entirely in the cyclotron 11/34).

3. Control software for data acquisition and plotting (split between all computers)
4. Smart control/monitoring software (entirely in the 11/45).

3.1 Control Software For Console And Cyclotron Hardware

The control software for the console and cyclotron hardware is based on a simple polling system. Every .1 seconds, the console program reads all of the console devices and updates the requested values in the multiport memory. Similarly, it reads the current cyclotron values from the multiport memory and updates the console displays from them. The cyclotron program has much the same function, but instead reads the cyclotron devices using them to update cells in the multiport memory, while using the requested values set by the console program to update the requests it makes of the cyclotron hardware. All console devices are incremental, this allows multiple console devices to be attached to the same cyclotron device without conflict, since the effects of change are simply cumulative.

3.2 Control Software For Data Acquisition And Plotting

Currently there are two devices which require plots to be made of beam current against a sensor position. These are the K-500 main beam probe which runs on a track from the central region all the way through the extraction channel giving current as a function of radius, and a K-500 viewer probe which gives a detailed beam profile in and near the extraction radius. The control software for these plotting devices is common and is broken up into three pieces, a data acquisition and control program, a data spooling program, and a plotting program.

The control and acquisition program runs in the cyclotron control 11/34. It is responsible for running the servos for both these probes and accumulating position and current measurements every 60'th of a second when plots are being produced. The data for these plots is buffered up in designated regions in the multiport memory. Position data is run through the appropriate calibration functions before being stored in the buffer.

The data spooling program runs in the 11/45 grabs the data buffers from the multiport memory and places it in a disk file. The spooler program then sends a message to the plotting program, which also runs in the 11/45, and tells it to read the disk buffer and plot it on a graphics terminal. The plots can later be dumped to a hardcopy device.

3.3 Monitoring And Smart Control Programs.

This is a set of programs which run in the 11/45 and either report the status of a set of devices, or control some devices in a manner not compatible with the control hardware. Space only permits a brief list of some of the programs which have been implemented in this group.

1. Control system log book generator -- This is a program which reads the control system multiport memory and produces a formatted page for inclusion in the K-500 logbook. The log book generator allows the operator to optionally include the latest set of probe traces along with the control settings.
2. Control system state saver -- This is a program which may be run to save the current control system values on a file. The file may be used later to reload the control system back to this state. This is a useful way to save optimal parameter settings for available beams.
3. Deflector Conditioner -- Conditions the electrostatic deflectors by running the voltages up at predefined rates until a current limit is exceeded, and then running the voltages back down.
4. Magnet logger -- Monitors the strain gauges, helium levels, currents and lead voltages for the K-500 cyclotron magnet (written by P. Miller).

4.0 CURRENT STATUS

At present, with the exception of the RF system, a good sample of the K-500 devices are computer controlled. In particular, the trim coils and their associated first harmonic steering bumps, as well as the extraction system. The R.F. may be turned on (warm started), the Dee voltages and relative phases may be altered or set, and pieces of the phase I beam line are also under control.

The control programs in the 11/45 add functionality which would not ordinarily be available in a hard wired control system. In particular, the plotting programs provide calibrated beam profiles at two important diagnostic regions, the system save/restore programs enable one to return reliably to a known good configuration, while the deflector conditioning program has saved many man hours of deflector conditioning by freeing the human operators from the tedious task of hand conditioning the deflectors.

A long road ahead remains however, the bulk of the K-500 R.F. system must be brought under computer control, as well as the majority of the

beam lines. Work on computer control of the experimental facilities has not yet even begun, and, of course, the K-800, and coupling line loom ahead as large systems which will require computer control.

5.0 CONCLUSIONS

The computer control system has proven useful providing, as it does, services beyond those which could be offered by hardwired analogs to the current control system. The strategy of keeping a picture of the 'state of the world' in a centrally located, multiaccess memory has greatly facilitated the development of the system by easing tremendously the communications problem typically faced by multiprocessor accelerator control systems.

UPGRADING THE TARGET LAB

L. Atkinson, S.J. Bricker, D.J. Morrissey,
J.A. Nolen, A.D. Panagiotou

We have devoted a good deal of effort to the modernization of the vacuum systems used in the target fabrication laboratory. In the past all the high vacuum pumping was done by oil diffusion pumps which had fallen into disrepair. As a first step in the modernization the rough pumping was consolidated into a single large pump with a manifold running the length of the room. There are three major pieces of vacuum equipment that are being upgraded, a filament evaporator, an electron beam evaporator, and a high vacuum target storage chamber.

The Veeco bell jar filament evaporator has been converted to a cryopumped system and is fully functional. We have begun to use this evaporator for the fabrication of target foils. Approximately 30 metal targets have been produced in the latter part of the year. A second bell jar system is currently being converted from diffusion pumping to cryopumping. This bell jar has been used to house a sputter source evaporator, in the future this bell jar will be used to house an electron gun evaporator. We plan to run two cold heads, one on each bell jar, from a common compressor. This system will bring us back to the point where the target maker can use one evaporation system while the other is pumping out.

The third piece of vacuum equipment that has been modernized is the high vacuum target storage chamber. It has been replumbed and connected to an ion pump. Previous experience with the diffusion pumped storage system has shown that the most serious problems are associated with power failures on the order of 5 to 30 minutes long. Such problems are minimized by ion pumps which continue to work for a short period after the power is turned off. The electronic control logic for removal of a target will be redesigned for the new system in the near future. In addition a new

high vacuum target transfer chamber has been designed which will allow transfer of air sensitive targets from storage to the target ladders of the S-320 and Enge spectrographs and the RPMS. The mechanism principally consists of a rotatable carousel for 20 target frames housed in a clear-walled portable chamber with a grabber for loading the target ladders. The design allows easy loading of both dry nitrogen-stored and high vacuum stored targets. Fabrication and assembly of the transfer chamber will be completed by the end of August of this year.

Many of the targets that will be used in experiments at the new cyclotron are substantially thicker than the traditional targets made by evaporation. It is not uncommon to use a 5 mg/square cm target at beam energies of 30 MeV/A. These targets are usually made by rolling a commercially available thick foil. We have obtained a small motorized rolling mill, International Rolling Mills Motorized Bench Model, in order to begin to roll target foils.

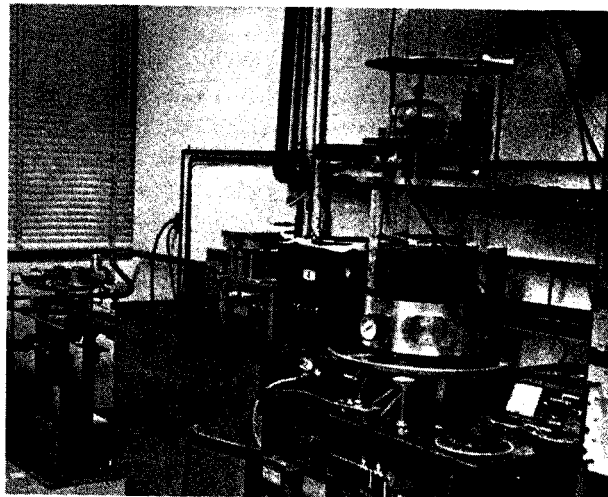


Fig. 1. Photograph of the target evaporation and high vacuum target storage areas.

L.H. Harwood, J.A. Nolen, Jr., and A.D. Panagiotou

Introduction:

The NSCL coupled cyclotron facility will provide intense (10^{12} part./sec) heavy-ion beams with E/A up to 200 MeV. Such beams will be of immediate use in answering many nuclear physics questions. They could also provide the laboratory with the ability to produce exotic beams (beams of $A\beta$ -unstable nuclei for nuclear physics experiments and/or one or two electron heavy atoms for atomic physics experiments) with useable intensities. Various methods of making "pure" exotic beams as well as various classes of experiments were addressed as to the apparatus needs for usefulness and their concomitant costs. Cost/benefit was investigated for each approach. Emphasis was placed on beams for nuclear physics use, but atomic physics needs were always kept in mind.

Physics with exotic beams:

Before one invests the funds which would be needed to make useable exotic beams (be they great or small), the types of experiments for which they could be useful should be enumerated. They break down into two basic classes: 1) experiments in which an exotic beam would increase the cross section and 2) experiments which are impossible without them. Some reaction mechanisms would have different examples which would fit into both classes.

Some fusion-evaporation experiments would fit into the first class along with exotic transfer reactions. A much-coveted nucleus is ^{100}Sn . Many attempts have been made to observe this doubly-closed nucleus, and all have failed; exotic projectiles might lead to a successful search. Gamma spectroscopy of several rare-earth nuclei would be possible for the first time with a proton-rich projectile. Very neutron-rich projectiles would make it possible to do gamma-spectroscopy on neutron-rich rare earth nuclei which were heretofore inaccessible by $(\text{HI}, \text{xn-yp-zY})$ reactions and would open these nuclei to study with the great range of experimental techniques which have been developed with stable beams producing neutron-deficient nuclei.

Exotic transfer reactions could have their cross-sections increased enormously. With a high quality beam, direct-transfer of four, five, or even six protons or neutrons would be possible with reasonable cross-sections. Systematics indicate that the $(^{20}\text{O}, ^{16}\text{O})$ reaction could have differential cross-sections as high as 1 mb/sr. The $(^{22}\text{O}, ^{16}\text{O})$ reaction could have a cross-section as high as 1 nb/sr, a small but not unuseable value provided there is sufficient integrated beam intensity. Again if the beam were of sufficient

quality, these reactions could provide ground state masses and level schemes of previously inaccessible nuclei.

Deeply inelastic transfer and fragmentation reaction mechanism systematics could be greatly expanded with exotic beams. The effects on both of the neutron number of the projectile could be investigated explicitly; at present there are few cases where one can study these reactions with more than one isotope of a given element. A logical part of the fragmentation studies would be a measurement of the effect of the neutron number of an isotope on its momentum distribution by measuring the longitudinal and transverse momentum distributions after these reactions.

Atomic physicists desire one- or two-electron atoms for their work. Their experiments are greatly improved as the Z of the atom increases; so a $91+$ U ion would thus be very attractive. To strip U to such a high charge state with useable intensity one needs to have an initial beam with E/A of several tens of MeV. The NSCL 40 Mev/u U beam would be quite good. If the exotic beam facility could separate different charge states of this beam (after going through a stripper) then atomic physics work of high quality could be done much more easily than with the much lower Z ions that are presently available.

This is certainly not an exhaustive list of the studies which would benefit from the availability of high quality exotic beams. Essentially any reaction that one can imagine doing with a stable beam would provide new information if these beams were available. Production of the beams and the actual feasibility of truly useful experiments is another matter. These will be addressed below.

Once the attractiveness of the secondary beams was established, we investigated various techniques for producing exotic beams of varying qualities and intensities. We also made counting rate estimates for many possible reactions. We reached two basic conclusions: 1) A dedicated secondary beam facility would be quite expensive ($\approx \$1.5$ M) and 2) many experiments would still not be feasible due to low counting rates. The former is due to the large emittance of the secondary beam and is increased by the need for experimental equipment to accommodate the large emittance of the beam. Examples of estimated counting rates (using reasonable target thicknesses and solid angles) are shown in table 1.

It was our conclusion that the large expenditures necessary to produce secondary beams would not be justified at this time. We alternatively proposed that the K800 extraction beamline be modified to provide low emittance (and, correspondingly, low intensity) secondary beams for evaluation prior to any long term decision.

Counting Rate Estimates Using Secondary Beams

Class	Example	Detected Rate(cps)
Direct Transfer	$(^{22}\text{O}, ^{16}\text{O})$	10^{-9}
	$d(^{24}\text{Ne}, ^{25}\text{Ne})p$	$10^{-3} - 1$
Fusion-Evaporation	$(^{36}\text{Ar}, x)$	10^{-6} (γ -rays/sec)
Deeply Inelastic Transfer		$10^{-3}/\text{MeV}$
Fragmentation		*

*Fragmentation feasibility established by Bevalac experiments since our secondary beam intensities could be as high as primary beams.

THE PRODUCTION OF 13-NITROGEN

D.J. Morrissey, J.A. Nolen, C. Purcell,
 J.M. Tiedje, G.P. Robertson, D.D. Myrold,
 A.J. Sexstone, and G.J. Mileski

We have adapted the nuclear reactions to produce 13-N to the new capabilities and limitations of the NSCL at MSU. In the initial series of experiments a 14-N beam was accelerated to energies in the range of 15 to 30 MeV/A and fragmented with a beryllium metal target to produce 13-N. The most likely product from the fragmentation reaction of 14-N with Be is 13-N with a lesser amount of 11-C being produced. The first goal of the studies was to establish the best bombarding energy for production of 13-N. Up to the present we have found the yield of 13-N increases with bombarding energy in the range of 210 to 420 MeV. Thus, up to the present capabilities of the k500, increasing the beam energy allows us to use thicker and thicker targets which have more than offset the declining beam intensities. Typical source strengths are on the order of a few microcuries of 13-N at beam intensities on the order of a few tens of nanoamperes. We hope to increase the beam intensity by at least one order of magnitude in the next operating period. The present source strength was sufficient to carry out the planned biological experiments. Additional source strength will allow us to perform treatments and replicates simultaneously.

In order to exploit the new production mechanism of 13-N we have developed an new target system for the irradiation station. The target system was designed to accommodate the fragmentation reaction used to produce the 13-N. The system uses a batch process for the production and delivery of the 13-N given the 10 minute half-life of the radiotracer. The target consisted of a beryllium foil, up to 1 mm thick. The reaction products are not stopped in the Be target but rather are allowed to exit from the target into an aqueous beam stop. The water facilitates conversion of the 13-N atoms into labeled nitrate and allows the rapid removal of the radioactive products from the accelerator vault but allows the production of unwanted 18-F along with additional amounts of 13-N and 11-C. An optimum Be target thickness will have to be calculated after the optimum bombarding energy is established so that the number of reactions in the water is minimized. Highly purified water was supplied from a closed system through a series of remotely controlled solenoid valves. The water supply and flushing was driven by helium pressure. A schematic diagram of the water system is shown in Figure 1. The Faraday cup water, approximately 1 cc, was flushed through the accelerator shielding in a

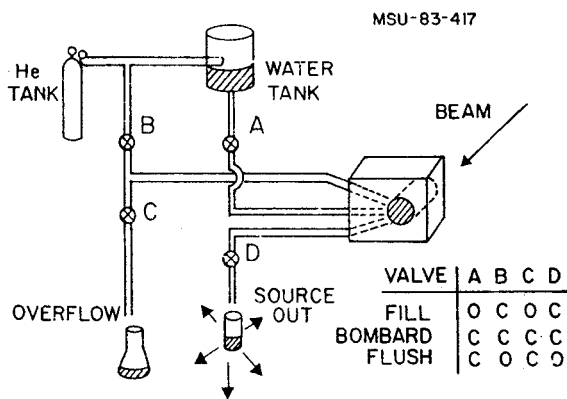


Fig. 1. A schematic diagram of the circulation system for the water that is the beam stop and radiotracer transport medium.

thin tube, approximately 20 m long, in 10 to 20 seconds after each production run. During the initial experiments we produced and used 13-N sources at the rate of about one batch per half hour. This rate of use of labeled nitrates was dictated by the data taking facilities not the cyclotron production.

In the next operating period we plan to continue increasing the bombarding energy in order to find the highest yield of 13-N. At that point we will optimize the yield of 13-N relative to 11-C by varying the Be target thickness, the beam intensity and length of bombardment. We will also explore the variation of the chemical form of the radiotracer on the bombardment history and makeup of the water collector. Prior to the next series of bombardments we are continuing to develop a CAMAC based data acquisition system suitable for radioactive decay studies. With the expanded capabilities of the new data taking system we will be better able to utilize the available beam time.

The following three types of biological experiments were done using the 13-N produced by the superconducting cyclotron.

a.) Measurement of natural denitrification rates.

Denitrification is the process whereby NO_3^- is converted to N_2 by specific types of bacteria widespread in nature. This process has been extremely difficult to study because of the difficulty of measuring the product, N_2 , in our atmosphere. 13-N provides the only direct way to measure this process without disturbing the natural atmosphere; the latter is important since O_2 is the major regulator of this process.

In our previous 13N studies we worked with soil slurries and microbial cultures, but we were never able to measure a natural denitrification rate because we could not trap $^{13}\text{N}_2$ in the presence of O_2 . Thus, we were incapable of studying denitrification in anything by anoxic environments. However, we have now built a thin

window proportional counter that allows us to measure a beta emitter in any atmosphere. Because this detector is inexpensive and can be used side by side with little "cross-talk", we have built eleven to allow us to do more replicates and treatments. The detectors are used in a recycling system in which soil atmosphere is pumped through a soil core as described in the last Annual Report. We have now shown that we can measure a denitrification rate with this new core method. Representative denitrification data obtained from a soil core are shown in Figure 2. Sterilized cores did not produce a labeled gas. The radioactive gas was confirmed to be $^{13}\text{N}_2$ by injection of a subsample through a gas chromatograph-proportional counter. We feel these results show that we can directly measure short term rates of denitrification under natural soil

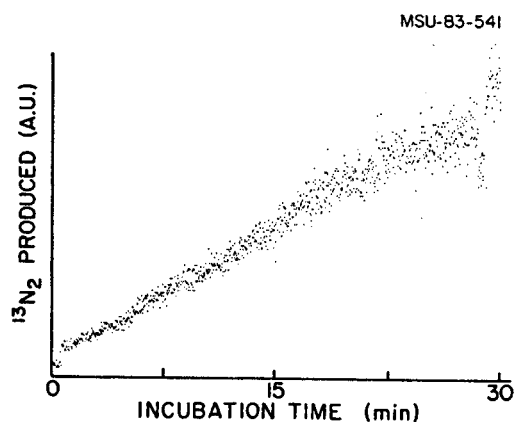


Fig. 2. $^{13}\text{N}_2$ gas produced from a forest soil core to which $^{15}\text{NO}_3^-$ was added in a simulated rain. Data were corrected for ^{13}N decay.

conditions, something not possible to do by other methods.

b.) Preliminary studies on $^{13}\text{NH}_4^+$ assimilation rates by natural microbial populations using ^{13}N . It is thought that NH_4^+ assimilation is an important dynamic flux of nitrogen but this cannot be measured by other means, e.g. ^{15}N , because of the large background of organic nitrogen. ^{13}N seemed well suited for studies of this process. The $^{13}\text{NO}_2^-$ and $^{13}\text{NO}_3^-$ produced by the cyclotron was converted to $^{13}\text{NH}_4^+$ by the standard MgO-Devarda's alloy reduction and steam distillation. This procedure also served as a purification step, removing residual traces of ^{11}C , ^7Be , and ^{18}F which are also produced by the cyclotron bombardment.

The $^{13}\text{NH}_4^+$ was added to slurries of Capac clay loam soil and incubated for 10 min. Two successive KCl extracts of the soil were performed to remove the inorganic nitrogen. These two extracts and the residual soil were counted using a NaI detector. The results obtained show that between 7 and 18% of the added $^{13}\text{NH}_4^+$ was removed

from the soil solution during the 10 min incubation and presumably assimilated by microorganisms (Table 1). Only 2 to 3% of the added $^{13}\text{NH}_4^+$ remained in the soil when a sterile control was incubated under the same conditions.

Table 1. $^{13}\text{NH}_4^+$ assimilation by the microbial population in a Capac loam soil.

Fraction	Nonsterile soil		
	Expt. 1	Expt. 2	Sterile control
	----- % of total label-----		
Total label added	100	100	100
1st filtrate	78	67	80
2nd filtrate	11	15	16
Extracted soil	6.7	7.8	2.2
Difference*	11	18	3.4

* Difference = Total label added - 1st Filtrate - 2nd Filtrate

The estimates of NH_4^+ assimilation were always lower in the extracted soil compared to the difference method because of differences encountered in geometry between the liquid and soil samples when using the NaI detector. This difference in geometry underestimates the total radioactivity in the soil. Despite this methodological problem, the overall results show that the dynamics of NH_4^+ assimilation in soil are rapid enough to be monitored using ^{13}N techniques. It will probably also be possible to measure rates of nitrification by ^{13}N but we have not yet investigated this process.

c.) Studies on the mechanism of the N-N bond formation in denitrification.

Microorganisms capable of denitrification have a heme containing nitrite reductase that converts NO_2^- to N_2O , but the mechanism of this key step in the nitrogen cycle has never been elucidated. Averill and Tiedje (1982) hypothesized that the sequence was: $\text{M} + \text{NO}_2^- \rightleftharpoons \text{M-NO}_2^- \rightleftharpoons \text{M-NO} + \text{NO}_2^- \rightleftharpoons \text{M-N}_2\text{O}_2 \rightleftharpoons \text{M-N}_2\text{O}_3^{2-} \rightarrow \text{N}_2\text{O}$. NO should also form NO^+ and eventually NO_2^- by the back reaction of the first dehydration. Establishing this back reaction of NO to NO_2^- is a key test of the hypothesis and can best be performed by using ^{13}N . In preparation for this experiment, we developed and tested a reaction to produce ^{13}NO , the substrate needed for the enzyme experiment. We produced ^{13}NO from $^{13}\text{NO}_2^-$ by reduction using KI , and verified that we had ^{13}NO by gas chromatography-proportional counting.

1. Averill, B.A. and J.M. Tiedje. 1982. FEBS Letters. 138:8.

D.J. Morrissey, S. H. Wernig and R. A. Blue

During the past year we have obtained a set of four 7.6 cm x 7.6 cm Bismuth Germanate (BGO) gamma-ray detectors. These detectors have a higher stopping power for gamma radiation than NaI(Tl) which is advantageous in heavy-ion reactions. The higher stopping power gives a larger photofraction for a given gamma-ray energy than in a NaI(Tl) detector of the same volume. However, one has to pay a price for this full energy absorption in light output and therefore in energy resolution and possibly in timing characteristics (for the presently available BGO material). The fact that the energy resolution with BGO is poorer than with NaI(Tl) is relatively unimportant in continuum gamma-ray studies, especially when compared to the improved full energy response. However, the timing characteristics of BGO are critical in determining its usefulness in heavy-ion reaction studies. The importance of the timing characteristics of the gamma-ray detectors used in heavy-ion reaction studies is easy to understand. The excited reaction products emit neutrons as well as gamma-rays, and the best method to discriminate between the neutrons and the gamma-rays is to measure the difference in their times of flight (over the same flight path).

We performed a simple experiment in order to establish the response of BGO detectors to fast neutrons from a Pu-Be source. This source emits a 4.4 MeV gamma-ray in coincidence with a 4 to 5 MeV neutron. The results of the neutron tests with 7.6 cm x 7.6 cm NaI(Tl) and BGO detectors are shown in figure 1. The pulse height created by the neutron is shown as a function of probability, normalized to the total number of neutrons expected to strike each detector. The curves are very similar in shape and magnitude. The only large difference occurs at low pulse heights where the probability of an interaction in NaI(Tl) is larger. If we integrate the spectra over pulse height, then we find that the probability of an interaction in the NaI(Tl) is 0.40 and in the BGO is 0.33, for the same unit volume. Thus replacement of NaI(Tl) with an equal volume of BGO brings with it a nearly equal neutron response.

Given the results of the neutron sensitivity study we will have to use time-of-flight techniques to discriminate between neutrons and gammas. The time resolution of the off-the-shelf BGO detectors is much poorer than that of NaI(Tl) detectors primarily due to the choice by the manufacturer of a photomultiplier tube (PMT) that optimizes energy resolution. We have found a PMT that can simultaneously optimize both the energy resolution and fast timing characteristics, the

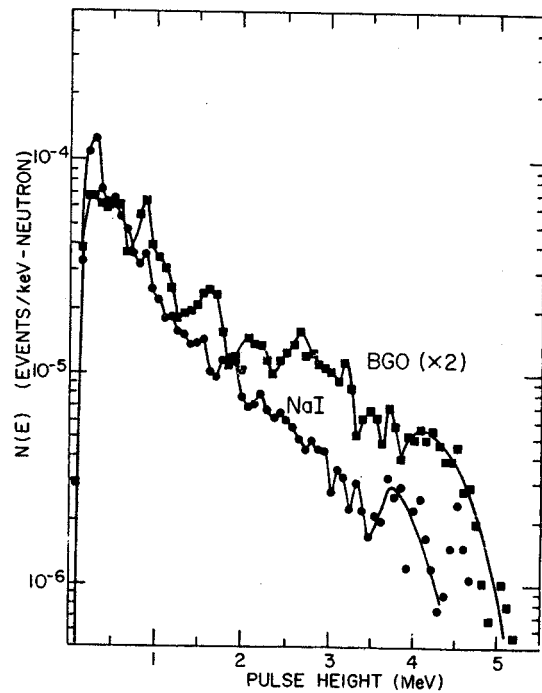


Fig. 1) Pulse height spectra of fast neutrons in BGO and NaI(Tl). The data have been normalized to the total fluence of neutrons, and the BGO data has been shifted up by a factor of 2 to separate it from the NaI(Tl) data. [MSU-82-371].

Amperex-2312B. The time resolution of BGO with the new tube was measured with a 60-Co source and in-beam. The results, 1.5 nanoseconds for 60-Co and 1.7 nanoseconds in-beam, represent the best rms time resolution obtained with BGO. These values are especially good in light of the relatively large volume of the detector.

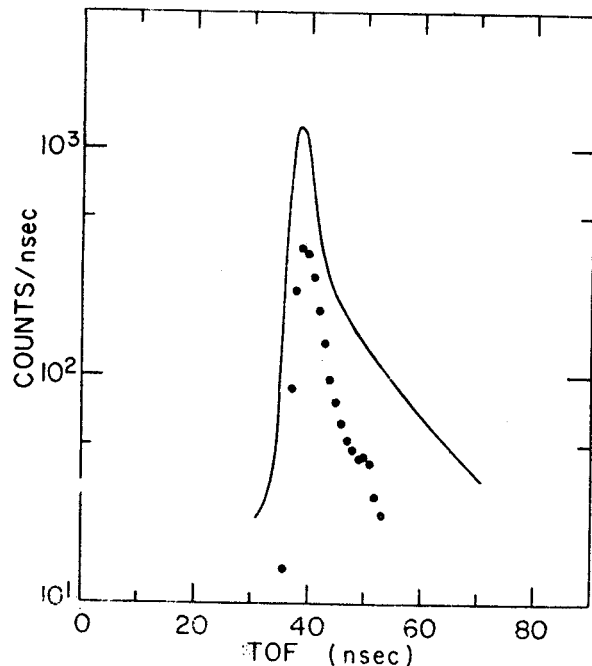


Fig. 2) The timing characteristics of a BGO detector coupled to an Amperex 2312B photomultiplier that were obtained with a 60-Co source (dotted curve) and in-beam (solid curve). [MSU-83-396].

TEST RESULTS OF TWO TIME-OF-FLIGHT
DETECTOR SYSTEMS

M.W. Curtin and J.S. Counseller

I. Introduction

In the event that isotopic separation is desired a viable option utilizes time-of-flight techniques where a minute energy loss triggers an electronic start signal and, at some predetermined distance, the particle intercepts a second detector thus producing an electronic stop signal. Coupled with a measurement of the total kinetic energy of the incident particle, one may ascertain the mass characteristic of the incident particle via the following relations:

$$T = \frac{1}{2} M_0 \frac{d^2}{t^2} \quad (\text{non-relativistic})$$

$$T = M_0 C^2 \left(\frac{1}{\sqrt{1 - \frac{d^2}{t^2}}} - 1 \right) \quad (\text{relativistic})$$

The largest uncertainty associated with mass resolution arises from the uncertainty in the measurement of the time required for the incident particle to traverse the distance between the start and stop detectors. The following relation indicates the expected mass resolution for a known time resolution:

$$2 \frac{\Delta t}{t} \sim \frac{\Delta m}{m}$$

Conventional wisdom indicates that $\Delta m \sim 0.7$ is sufficient to separate individual masses. Decreasing Δt has several advantages. One example, particular to the experiment prompting this testing endeavor, utilizes the following line of reasoning. The relevant maximal energy and maximal mass measurements are dictated from the theory thus if it is possible to reduce Δt , the uncertainty in the time measurement, a corresponding decrease in t , the time-of-flight, is possible, hence for fixed maximal energy, the flight path length can be safely reduced thus increasing the available solid angle.

Two time-of-flight systems were tested. A basic description of the systems and underlying principles and test results are presented.

II. Time Zero Detector

The time-zero-detector (TZD) was designed to operate in the S320. The start detector consists of a WE102 scintillator enclosed in a hemispherical mirror which improves the light gathering capabilities of the system. A cross sectional perspective of the TZD is provided in Fig. 1. In the interest of clarity, the time sequence of events proceeds thus: 1) the particle enters the front aperture of the hemispherical mirror 2) the particle traverses the scintillator liberating photons which are collected either

directly by the photomultiplier (P/M) or are reflected by the hemispherical mirror to the P/M 3) the particle exits via the rear aperture and proceeds to the stop detector. The second comment of the preceding sentence illustrates an inherent indeterminacy in the time measurement since the direct and reflected path lengths vary. To reduce

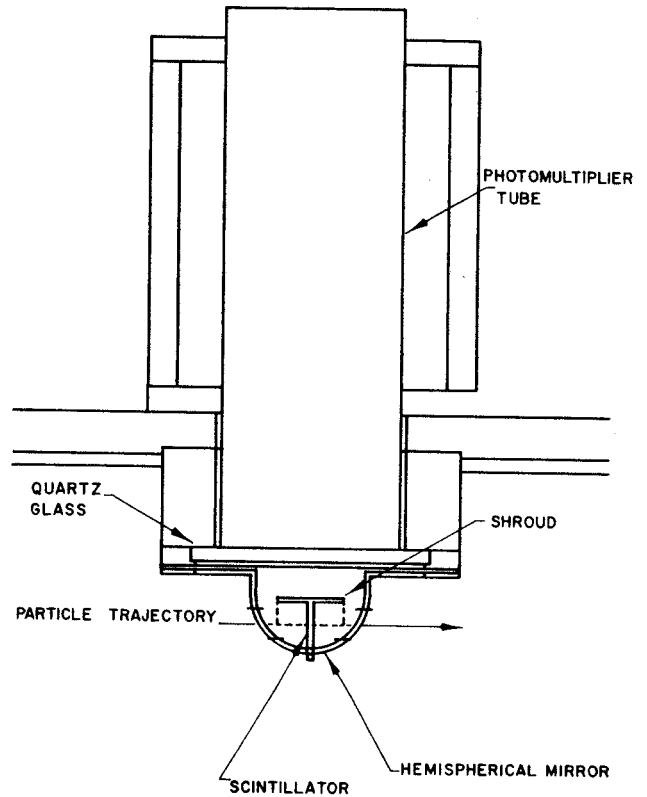


Fig. 1.

this contribution, a removable shroud was inserted to reduce the direct contribution thus preserving some of the advantages of good collection efficiency while reducing the uncertainty in the time measurement. The mirror was constructed by a vacuum form molding technique applied to plexiglass. An epoxy paint was applied to the interior surface of the mirror after the entrance and exit apertures were drilled. This insures a smooth surface to evaporate the silver upon. The entire device is mounted in one of the large, top portals in the Minnesota chamber wedge.

A schematic of the electronics used in the test apparatus is illustrated in Fig. 2. The stop detector was a 1500 μ solid state detector and a ^{241}Am source served as an alpha emitter. The procedure requires two measurements with different delays which allows one to determine the channel to time conversion for the MCA (multi-channel analyzer) output. Utilizing the conversion and the full width at half maximum (FWHM) of the individual TAC (time to amplitude converter) peaks, one can determine the uncertainty in the

time measurement. The result was $\Delta t \approx 1.8$ nanoseconds.

MSU-83-556

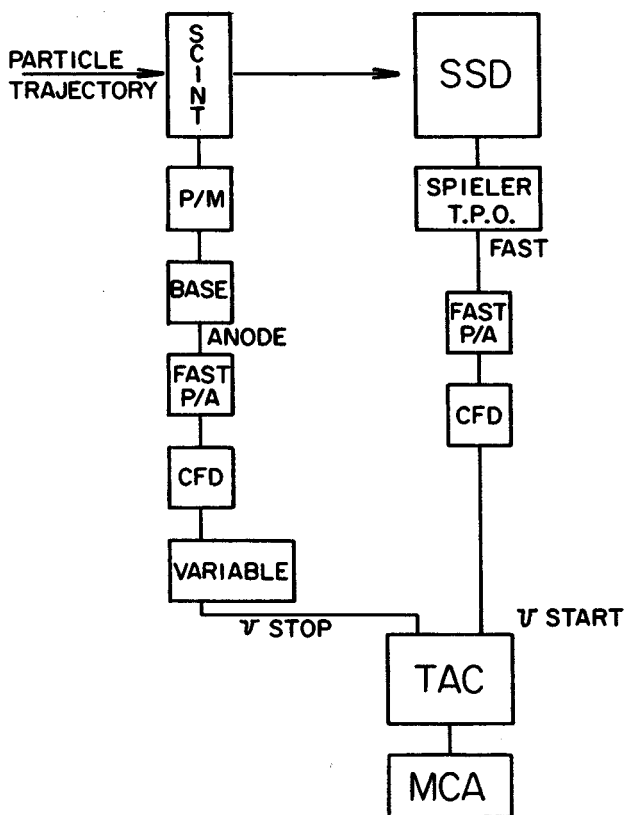


Fig. 2.

Some suggestions regarding improvements of the testing apparatus are:

- 1) Use a thin, small area transmission type solid state detector.
- 2) Use a thinner source to minimize inherent straggling of the emitted alpha particles.

II. Microchannel Plate Assembly

The Argonne Microchannel Plate (MCP) assembly consists of a Carbon foil which the incident particle traverses (with minimal energy loss) thus liberating electrons from the foil, as illustrated in Fig. 3. Accelerating grids (not shown in Fig. 3), accelerate the electrons which are coerced into a curved trajectory due to the presence of a uniform magnetic field. The paths are isochronous thus preserving the small timing uncertainty. The electrons then impinge on the MCP directly which is an electron multiplier. The important feature that readily lends this assembly to accurate TOF determinations is that the electron multiplying material is drawn into long, narrow filaments

which are subsequently surrounded by an insulating material thus channeling the cascading electrons into narrow paths hence preserving the small inherent time dispersion due to path length variances.

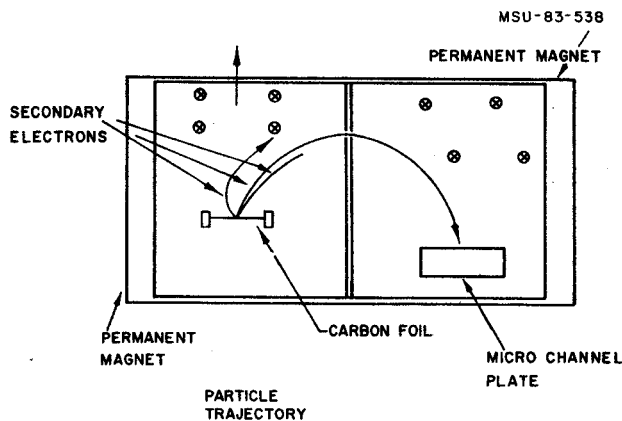


Fig. 3.

A ^{212}Po source was used to supply alpha particles. A 75μ solid state detector served as a stop detector. Rise times were approximately 600 ps with a corresponding efficiency of $\sim 60\%$ for the 8.8 MeV alpha particle. The source used in the test apparatus (illustrated in Fig. 4), emits two alphas of different energy and since the time difference for the two particles to traverse the flight path was $\sim 200\text{ps}$, commensurate with the resolution of the system, it was necessary to gate on the energy signal via the slow line indicated in Fig. 4. The result obtained was $\Delta t \sim 250\text{ps}$.

MSU-83-557

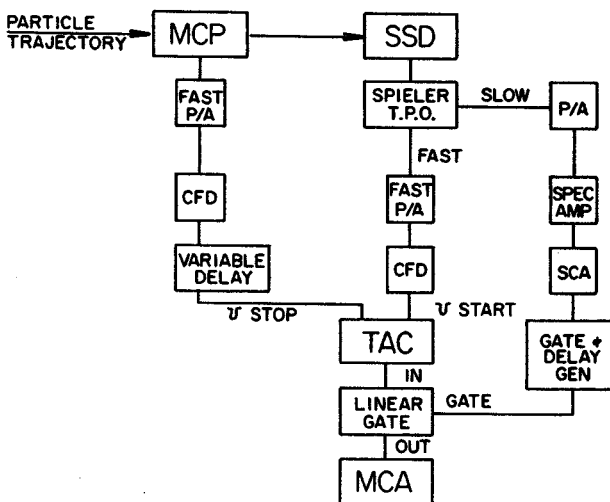


Fig. 4.

PROTOTYPE HIGH ENERGY NEUTRON MONITOR

E. Kashy, B. Remington, and J. Yurkon

A prototype neutron detector for the phase II radiation protection system has been constructed and is now in the initial testing and evaluation stage. It consists of a 5" x 5" cylinder of Ne 110 plastic, attached with a UVT light pipe to a 2 inch photomultiplier tube. The planned use of these detectors is to obtain an on line signal of the dose rate due to the high energy neutrons, i.e., neutrons of energy 30 MeV and above. Such detectors would be used in addition to the highly moderated BF gas proportional counters in the current radiation protection system.

Figure 1 shows the background spectrum in the prototype detector taken over a 19 hour period. The peak in the spectrum at above 20 MeV is caused by minimum ionizing muons traversing the scintillator. A thorium source was used to calibrate the detector's response.

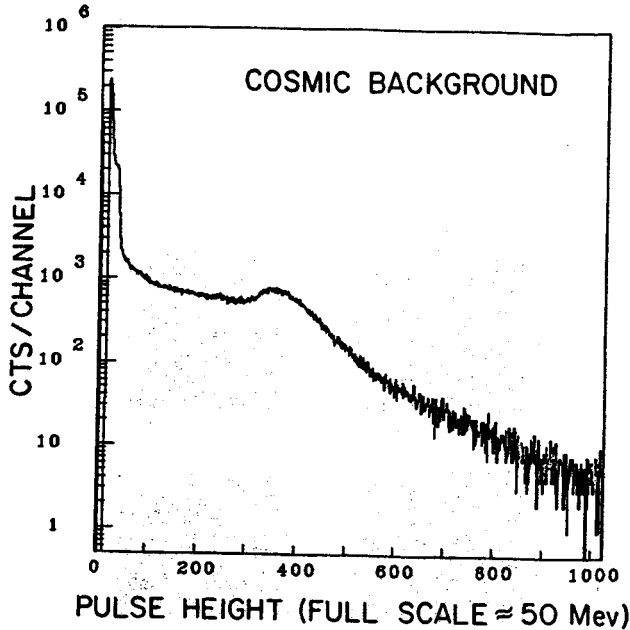


Fig. 1.

The efficiency of the detector for high energy neutrons can be calculated from knowledge of the cross section of the (n,p) on the hydrogen and (n, α) on the C content of the scintillator,

and of the response function of the scintillator for the p and the ^4He . The computer code of Cecil et al. from Kent State University which uses Monte Carlo method of calculation has been used for 2.5" x 2.5", 5" x 5", and 7.5" x 7.5" cylindrical scintillators. A sample result for the 5" x 5" scintillator for 200, 100, and 50 MeV neutrons is shown in Figure 2, with the neutrons directed along the axis of the cylinder. The neutron detection efficiency is plotted as function of equivalent electron light output threshold. The usefulness of this detector for the purpose of high energy neutron dosimetry looks good so far. As can be seen from fig. 2. the detection efficiency is approximately independent the neutron energy for a threshold setting of 10 MeV.

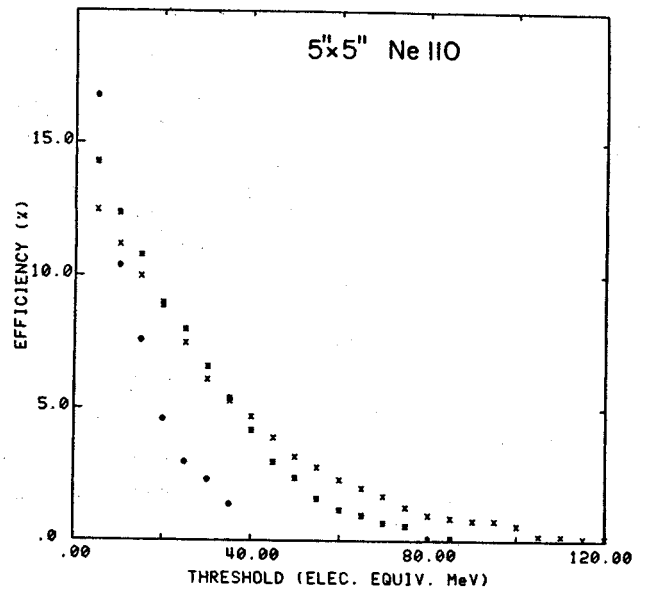


Fig. 2.

This is ideal for monitoring since for this neutron energy domain, the neutron flux for a given dose is also nearly energy independent, with $4 \text{ n/cm}^2\text{-sec}$ resulting in a dose of 1 mrem/hour. The feature that its operation can be monitored by its cosmic ray response, insures that the detector is properly operating at all times. Design of the necessary circuitry and logic for the operation of the detector and integration in the safety system will begin soon.

M.I.W. PROPORTIONAL COUNTER

K. Beard, W. Benenson, E. Kashy, B. Sherrill,
J. van der Plicht, J. Yurkon

Experiments to measure the pion energy spectrum from (HI, π^{\pm}) reactions below the nucleon-nucleon pion production threshold using the Enge split pole spectograph require the development of a new multiwire gas proportional counter. This detector has been designed to solve two problems; 1) the very high background which is expected from the high intensity high energy beam and 2) the 45° incidence angle on the focal plane which makes the conventional MWPC configuration cumbersome.

The multi-inclined wire (MIW) counter solves these problems by positioning the wires along the trajectory direction (fig. 1). The energy loss

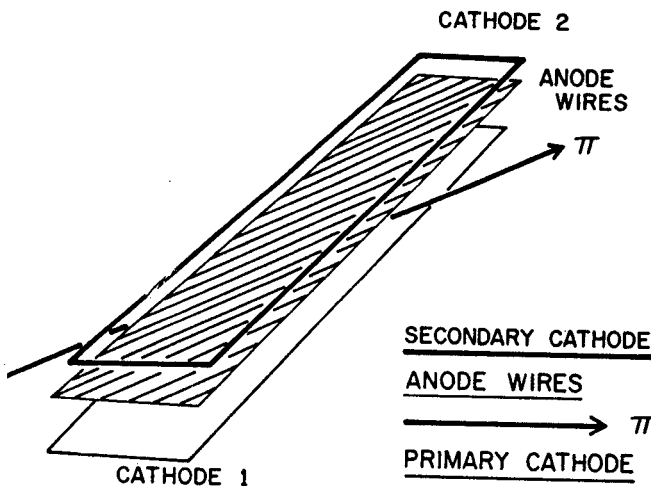


Figure 1

signal from the nearly minimum ionizing particle is therefore optimized relative to the randomly directed background events. At most three wires can fire, which is an appreciable improvement over the nine expected from the conventional MWPC configuration at 45° incidence. MWPC's in general are required to minimize the active volume per output channel. In other words a single wire counter would have a raw counting rate (all background) in the preamp 100 times larger than each wire of a 100 wire MWPC. The new LeCroy PCOS III system will connect each anode wire to its own amplifier/discriminator and hence to CAMAC and the VAX 750.

Tests on the prototype (MIW II) suggested changes which were incorporated into a second prototype (MIW III, fig. 2). This prototype has two wire planes of 16 active wires each, one plane in front of the other, with a wire spacing of $0.1414''$, a primary cathode-anode gap varied between $.374''$ and $.787''$, a secondary cathode-anode

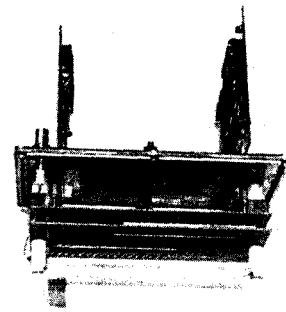


Figure 2

gap of $.062''$, and $.005''$ dia. gold plated tungsten wires. Typical operating parameters were -5.5 KV on the primary, -1.89 KV on the secondary, in 1 atmosphere of 50-50 argon-ethane. Using a collimated Ru-106 source (3.54 MeV electrons) and a primary gap of $.787''$, the spectra in shown fig. 3 were obtained. About 98% of the time only one or two wires fired, and the position resolution seemed to be limited by multiple scattering of the electrons in the gas (fig. 3).

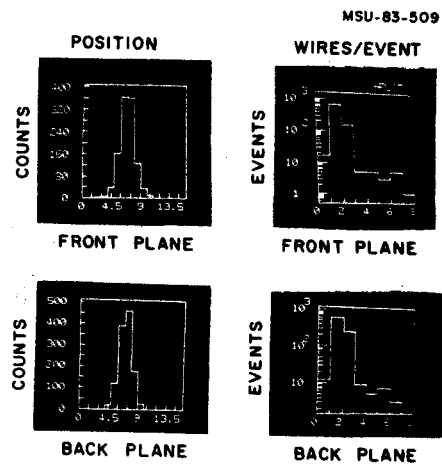


Figure 3

The final design of the gas box has two wire planes, centers separated by $1.125''$ (fig. 4). The primary cathode gap is $.787''$, the secondary $.062''$. Each plane contains 96 active wires, each of which connects to its own amplifier on a 16 channel card mounted on the outside of the gas box. The MIW is active along $19.2''$ of the focal plane, and has an overall length of $28.9''$ (fig. 5). A typical energy range is 20 to 36 MeV pions.

The PCOS III 2735 cards require air cooling, and hence the detector and cards are mounted in the camera box which is open to air. A $.003''$

kapton window across the exit of the split-pole maintains vacuum inside. On the exit side of the MIW gas box will be a delta-E scintillator, .25" thick, and an E scintillator, 3.00" thick. Both are made of Bicron BC-408 plastic, with Plexiglas UVT lightpipes and RCA 8575 photomultipliers at either end.

The scintillators and the gas box will be mounted on a common aluminum plate, with room for an interchangeable wedge to be placed between the

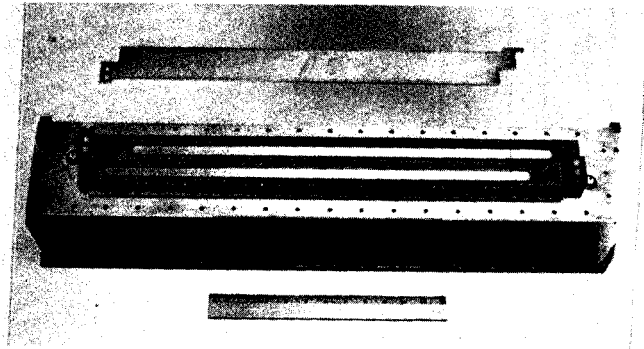


Figure 4

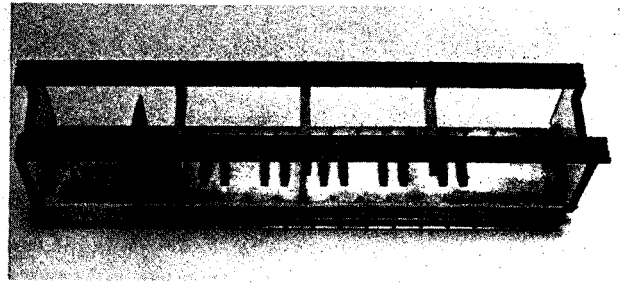


Figure 5

box and the delta-E scintillator. At pion energies above about 100 MeV, a wedge is used to keep the pions stopping in the E scintillator.

The magnetic fringe field in the camera box is considerable (~40 gauss) and so shielding for the phototubes was designed. Two cylindrical shields protect each phototube, the outer of .060" thick 1018 steel, the inner of .060" annealed MuShield.

J.E. Yurkon, C.K. Gelbke, W. Lynch

Low pressure multiwire proportional counter's (MWPC's) have proven to be highly accurate timing and imaging detectors. MWPC's operating in the 0.3 to 10 Torr range have demonstrated position resolutions of $100 \mu\text{m}$ (FWHM) and timing characteristics of 135 nsec. for heavy ions¹. MWPC's offer advantages over conventional Position Sensitive Avalanche Detector's (PSAD's). MWPC's offer higher gain than PSAD's at equal reduced fields. Since they can be operated at extreme E/P the positive ions are removed very rapidly and allows operation at counting rates of the order of $10^5/\text{S mm}^2$.

The method of delay line readout is shown schematically in Fig. 1 (extracted from Ref.1). The avalanche on the anode-wire plane induces

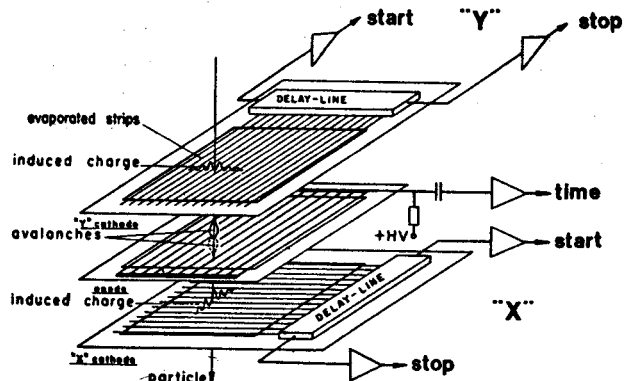


Fig. 1. Delay line readout of MWPC's.

charge on the Cathode readout stripes. Since the induced charge covers several stripes the position is interpolated by the delay line readout. The width of the stripes is 5 mm and the space between stripes is 0.5 mm. The position is read out by measuring the time between the anode start pulse and the delay line output. The counters use 4 delay lines (2 for each axis) of the type T2B12-5²). They have a characteristic impedance of 50 Ω 's and a delay of 2 nsec's per tap. The foils are spaced 3 mm from the anode. The anode is made of 12 μm wires spaced 1 mm apart. The total active area of the detector is 11 cm x 11 cm. Cross sectional view is shown in Fig. 2. The detector has been constructed without the need for an external gas box. This greatly simplifies assembly and reduces the cost significantly. The assembled detector is shown in Fig. 3.

Tests of the MWPC have been made using a CF 252 Fission source and a Am^{241} α source. Two identical detector were placed 6 cm. apart. A mask with 800 μm and 300 μm hole was used to

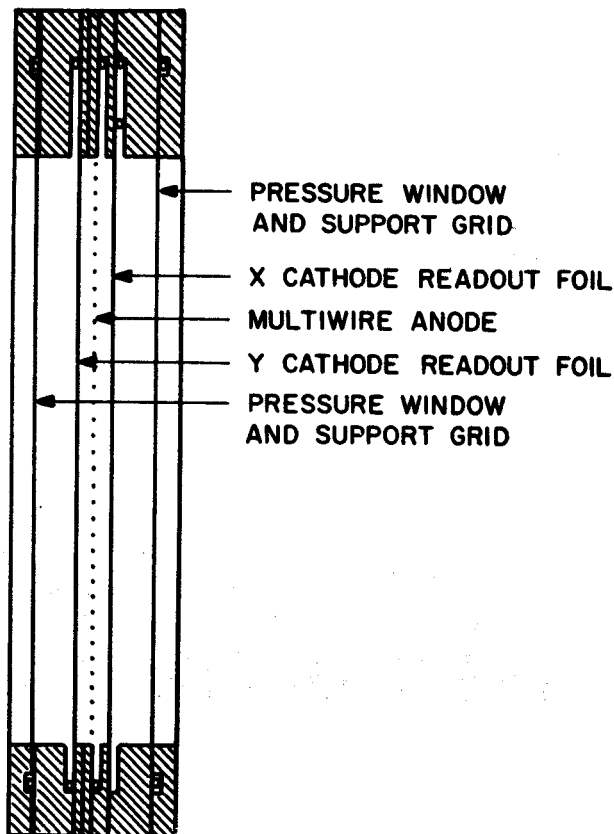


Fig. 2. Construction of low pressure MWPC's.

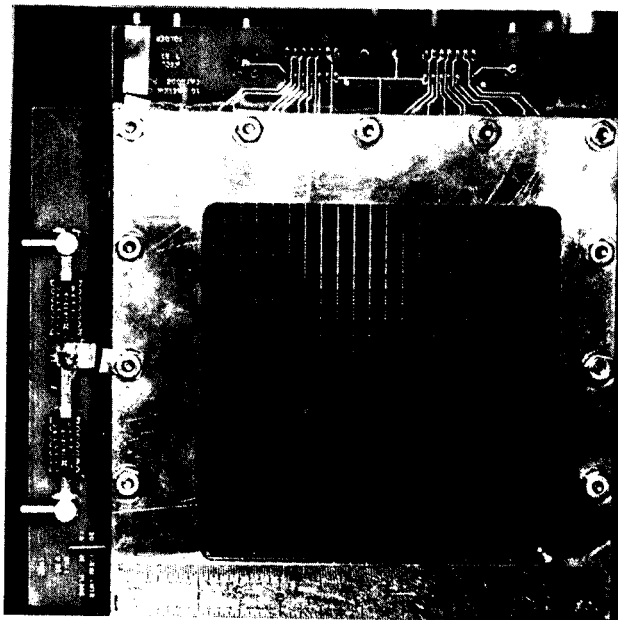


Fig. 3. View of assembled MWPC's.

collimated the CF source. Figure 4 shows a position spectrum taken at 4 torr of isobutane and on operating voltages of 510 volts. The 800 μm holes gave FWHM of 900 μm to 500 μm depending on the orientation of the hole to the source. The

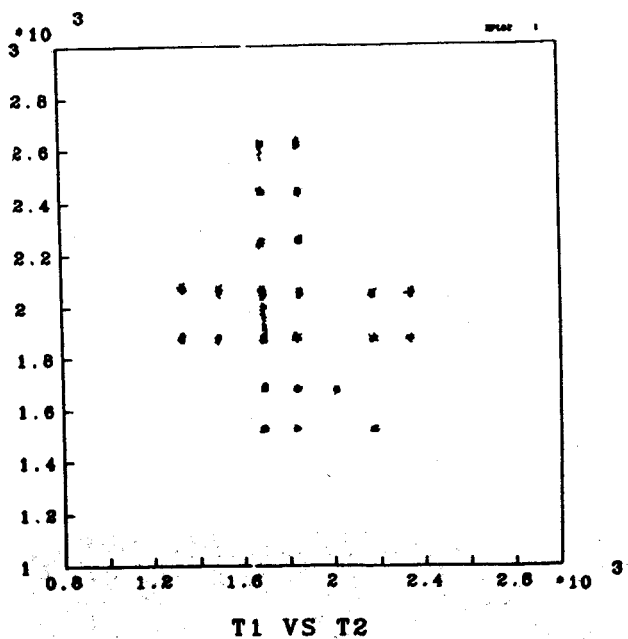


Fig. 4. Histogram of position spectra.

300 μm holes after 24 hrs. of counting had insufficient statistics. Since the holes were lined up however, we made a projection and this gave a FWHM of 600 μm . Thus we have an apparent resolution of 500 μm FWHM. Figure 5 shows a time of flight spectrum of the fission fragments over 6 cm. The faster group has a FWHM of 980 psec's. This is not corrected for kinematics. Operation at 6 torr of isobutane and 615 volts gave a time resolution of 1.7 nsec's for Am^{241} α 's. This

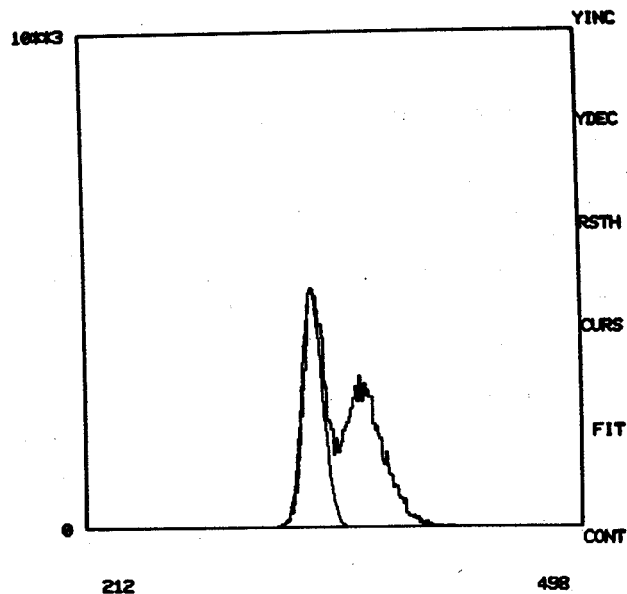


Fig. 5. Time of flight spectra of CF_{252} . 74 psec's/channel.

appeared to be roughly 4 times the limit that may have been obtainable had we not been operating in a strong area of RF interference. This is consistent with previous measurements³⁾.

The low pressure MWPC's promise to be a low cost, large area start detector with excellent position accuracy and solid angle efficiency.

1. A. Breskin, WIS-53/82 Nov-Ph (1982)
2. Manufactured by Rhombus, Inc.
3. A. Breskin, R. Chechik, and N. Zwang, Nucl. Instr. and Meth. 165 (1979) 125

A LOW NOISE CHARGE INTEGRATING AMPLIFIER FOR USE
IN ION CHAMBERS

J. Yurkon, W. Lynch

High resolution Ion chambers are often limited by the intrinsic noise of the associated electronics. The preamplifier is the most critical stage of signal processing. For small ion chambers of low capacitance the coaxial cables connecting the preamp present an unnecessary burden. It was therefore decided to build a small preamplifier that could be mounted inside the ion chamber.

Designing a low noise preamp calls for special attention to the first active gain element. After the first stage is properly designed it is difficult to go wrong. The usual choice for a gain element for an ion chamber is an FET. This is because the noise current for an FET is six orders of magnitude less than for a Bipolar Transistor. The noise current is important because an ion chamber is low capacitance detector usually used with microsecond peaking times and this implies a high impedance device making I_n^2 s significant¹⁾. For RC-CR time constants usually used in shaping the signal the noise voltage (E_n) predominates over the noise current (I_n) so that the FET selection should be based on its E_n should be the deciding criteria. A siliconix 2N5434 FET was chosen. Figure 1 shows the equivalent input

Integration yields 1.4×10^{-16} C FWHM for a total capacitance of 30 pf. i.e. the Fet gate capacitance. This implies an energy resolution of 2.6 KeV in silicon.

The Fet is biased by an Fet constant current source. This removes the possibility of noise being coupled in from the nim power. The following amplification stage is a Lecroy TRA 1000 monolithic amplifier. A charge feedback capacitance of 2.2 pf is used. The emitter follower output of the TRA 1000 proved to be too slow for positive input pulses so the internal bias resistor was bypassed to put the bias current of the transistor into a region where it could be operated satisfactory. The entire assembly is quite small as shown in figure 2. Tests of the

Equivalent Input Noise Voltage and Noise Current vs Frequency

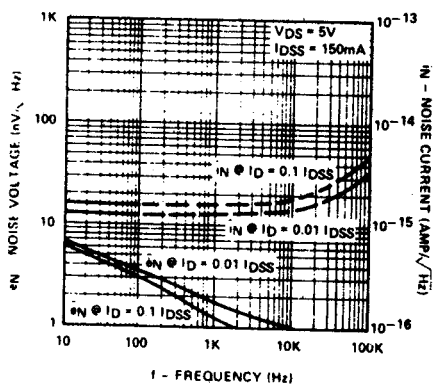


Fig. 1. Equivalent input noise of 2N5434

noise voltage on this FET. The input noise after RC-CR shaping is given as

$$\frac{E^2}{C^2} = \frac{e^2}{8} \int_0^\infty e_n^2 \{G(f)\}^2 df$$

where

$$G(f) = 2\pi f T_0 / (1 + 4\pi^2 f^2 T_0^2)$$

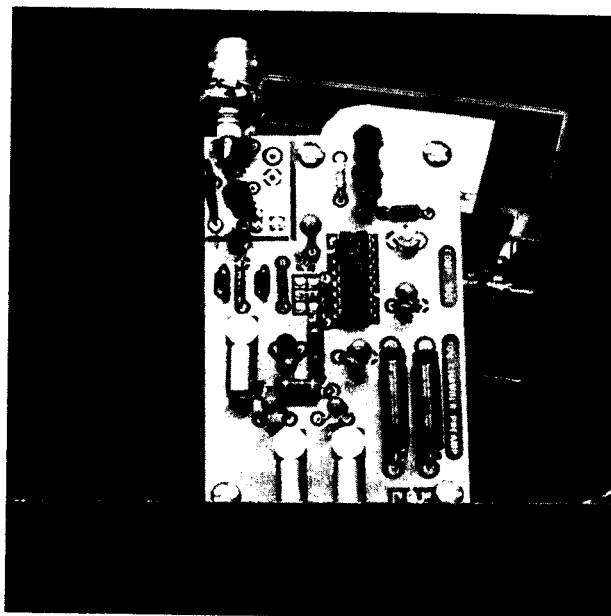


Fig. 2. View of assembled preamplifier

preamp show a linearity of 0.27% over a 40 MeV range. The noise figure for a 1 microsec RC-CR shaping time is measured to be 2.7 KeV in silicon as predicted. The amplifier can easily be modified for larger dynamic ranges, or current modes of operation.

1. H. Spieler, I.E.E.E. Trans. Nucl. Sci. NS-29, Ho. 3 (1982) 1142
2. F. Goulding and D. Landis I.E.E.E. trans. Nucl., Sci. NS-29, No. 3 (1982) 1125